ADVANCING EARTH AND SPACE SCIENCE

Geophysical Research Letters

RESEARCH LETTER
10.1029/2019GL085837

Key Points:
- Goddard Earth Observing System-Massachusetts Institute of Technology general circulation mode is able to reproduce past observed sea surface temperature (SST) and wind stress correlations
- Analysis of higher temporal resolution SST and wind speed reveals several days SST wind speed cycle
- We suggest a mechanism for the cycle

Supporting Information:
- Supporting Information S1

Correspondence to:
E. Strobach,
strobach@umd.edu

Citation:
Strobach, E., Molod, A., Trayanov, A., Forget, G., Campin, J.-M., Hill, C., & Menemenlis, D. (2020). Three-to-six-day air-sea oscillation in models and observations. *Geophysical Research Letters*, *47*, e2019GL085837. https://doi.org/10.1029/2019GL085837

Received 14 OCT 2019
Accepted 13 MAR 2020
Accepted article online 22 MAR 2020

Three-to-Six-Day Air–Sea Oscillation in Models and Observations

Ehud Strobach[1,2], Andrea Molod[2], Atanas Trayanov[2,3], Gael Forget[4], Jean-Michel Campin[4], Chris Hill[4], and Dimitris Menemenlis[5]

[1]Earth System Science Interdisciplinary Center,University of Maryland, College Park, MD, USA, [2]Goddard Space Flight Center, Greenbelt, MD, USA, [3]Science Systems and Applications Inc., Greenbelt, MD, USA, [4]Massachusetts Institute of Technology, Cambridge, MA, USA, [5]Jet Propulsion Laboratory,California Institute of Technology, Pasadena, CA, USA

Abstract Analysis of coupled ocean-atmosphere numerical simulations revealed a widespread oscillation of sea surface temperature (SST) and surface wind anomalies with a cyclic nature characterized by a period of 3 to 6 days. Similar oscillations were also found in buoy data at different locations around the globe and in an atmospheric reanalysis, albeit the oscillations were noisier and stronger in the observations, and they were weaker and longer period in the atmospheric reanalysis. These oscillations did not, however, develop in an atmosphere-only simulation, suggesting the importance of ocean–atmosphere coupling for simulating this phenomenon. We propose a mechanism for this interaction involving a feedback between SST and surface wind.

1. Introduction

Earth system models suffer from prediction errors and biases, especially but not exclusively in the vicinity of the air–sea interface (Intergovernmental Panel on Climate Change (IPCC), 2013). Several recent studies have described feedbacks (or interactions) between the atmosphere and the ocean that may both play important roles both in terms of understanding dynamical processes in the earth system (e.g., Chelton & Xie, 2010; Ma et al., 2016; Zebiak, 1993) and in terms of prediction skill (e.g., Alexander et al., 2002; Kirtman et al., 2012; Richter, 2015; Rodwell & Folland, 2002). The consequences of misrepresenting air–sea feedbacks on surface fluxes have negative impacts for the major uncoupled atmospheric and oceanic reanalyses and state estimates (Balmaseda et al., 2015; Valdivieso et al., 2017). Some of the consequences of missing air-sea feedbacks were discussed in Strobach et al. (2018). Investigating air-sea interactions and identifying the cause for the lack of fidelity in their representation in climate models may, therefore, have important implications. The present study identifies and investigates a widespread oscillation of sea surface temperature (SST) and surface wind anomalies with a cyclic nature characterized by a period of three to six days.

Studies using coarse-resolution observationally based products generally found a negative correlation between SST and surface wind speed (or wind stress) anomalies at monthly time scales (Liu et al., 1994; Mantua et al., 1997; Okumura et al., 2001; Xie, 2004). This interaction between the ocean and the atmosphere was interpreted as the ocean passively responding to wind-induced latent and sensible heat fluxes (Liu et al., 1994). More recent studies have focused on air-sea feedbacks caused by the presence of oceanic mesoscales, whereby wind speed anomalies are stronger over warm ocean anomalies and vice versa (Chelton et al., 2001; Chelton & Xie, 2010; Hashizume et al., 2001; Liu et al., 2000). The most common explanation for the positive correlation is that positive SST anomalies increase planetary boundary layer (PBL) instability and the resulting turbulence acts to transfer momentum from upper atmospheric levels to the surface (Chelton & Xie, 2010). This is similar to air-sea feedback mechanisms that have been used to explain the propagation of tropical instability waves (Hayes et al., 1989; Wallace et al., 1989). Positive correlations between SST and wind speed anomalies were also reported in the modeling study of Bryan et al. (2010), who found that positive correlations only occur when the ocean model is configured with horizontal grid spacing that can admit mesoscale eddies.

There is a growing number of modeling studies that demonstrate the effect of mesoscale ocean features (e.g., mesoscale eddies and western boundary currents) on the atmosphere. Most of these studies, however, were carried out using atmosphere-only models. Some studies showed local effects on the atmosphere such as changes in the cloud properties and rainfall (e.g., Frenger et al., 2013; Liu et al., 2018; Small et al., 2008).

10.1029/2019GL085837

Others demonstrated the influence of ocean mesoscale eddies on large-scale atmosphere phenomena, such as atmospheric blocking, storm tracks, and monsoon rainfall (e.g., Farneti et al., 2010; Foussard et al., 2019; Kuwano-Yoshida & Minobe, 2017; Matsueda et al., 2009; Ma et al., 2015, 2017; Zappa et al., 2013).

Studies of air-sea interactions that examined the relationship between SST and wind speed anomalies mainly focused on regions with strong mesoscale ocean features, for example, western boundary current extensions, the Antarctic Circumpolar Current (ACC), and tropical instability waves. These features are all associated with sharp spatial SST gradients, have horizontal scales of 10 to 1,000 km, and decorrelation time scales larger than 30 days. Analysis of observations and model data with temporal resolution of a month or more are adequate to resolve these scales of ocean variability, and, indeed, most of the previous studies have focused on those longer time scales. However, the time scale at which the atmosphere interacts with the ocean is expected to be considerably shorter than the 30-day life cycle of the ocean mesoscale features discussed in these studies. Additionally, the spatial scale of the interactions is expected to be closer to the scale of smaller ocean mesoscale eddies. Investigating shorter time and space scales may provide us with insights on how the atmosphere responds to oceanic changes and whether the response is part of ocean-atmosphere feedback loops. In this study, we analyze coupled and uncoupled ocean-atmosphere simulations, atmospheric reanalysis results, and buoy observations using daily temporal sampling in order to explore the potential for high-frequency (submonthly) atmosphere-ocean feedback mechanisms.

2. Materials and Methods

During the past few years, the model development groups of the Goddard Earth Observing System (GEOS) atmospheric model and the Massachusetts Institute of Technology (MIT) general circulation model (GCM; MITgcm) ocean model have produced, respectively, global atmosphere-only and ocean-only simulations with kilometer-scale grid spacing. These simulations have proved invaluable for process studies and for the development of satellite and in situ sampling strategies. Nevertheless, a key limitation of these “nature” simulations is the lack of interaction between the ocean and the atmosphere, which limits their usefulness for studying air-sea interactions. To remove this limitation, the two modeling groups have worked to couple the GEOS atmospheric GCM (AGCM) to the MITgcm ocean model in order to produce high-resolution coupled simulations.

We briefly describe the particular configurations of these two models as they are used in our study. The GEOS AGCM's dynamical core and suite of physical parameterizations is described in detail in Molod et al. (2015) and in Gelaro et al. (2017). In this study, the surface parameterization of turbulent fluxes is a modified version of the parameterization documented in Helfand and Schubert (1995), with a wind stress and surface roughness model modified by the updates of Garfinkel et al. (2011) for a midrange of wind speeds, and further modified by the updates of Molod et al. (2013) for high winds. The GEOS AGCM's cubed-sphere grid was configured to run with nominal horizontal grid spacing of 14 km. The vertical grid type is hybrid sigma-pressure with 72 levels. MITgcm has a finite volume dynamical core (Marshall et al., 1997). It has a nonlinear free-surface and real freshwater flux (Adcroft & Campin, 2004) and a nonlocal K-profile parameterization scheme for mixing (Large et al., 1994). The MITgcm grid type is the so-called “Lat-Lon-Cap” (Forget et al., 2015), and it was configured to run with nominal horizontal grid spacing of 4-9 km. The vertical grid type is the z^* height coordinates (Adcroft & Campin, 2004) and it has 90 vertical levels.

The GEOS-MITgcm atmosphere-ocean interface includes a skin layer model (Price et al., 1978), configured for the simulations described here to impose an hourly time scale on the interaction, and the communication between the ocean and atmosphere is updated at every atmospheric model time step (3 min). In atmosphere–ocean GCM (AOGC) mode, the SST is the temperature of the skin layer. When running in AGCM mode, GEOS uses the atmosphere–ocean interface layer of Akella et al. (2017), which allows the lower boundary condition for the atmosphere to differ from the values prescribed in the ocean temperature data set, and includes a sensitivity of the SST to the surface winds. In this mode, the SST is the lower boundary condition of the atmosphere.

Three different high-resolution experiments were carried out: (i) ocean-only (OGCM), (ii) atmosphere-only (AGCM), and (iii) coupled atmosphere–ocean (AOGCM). The OGCM experiment was of 6-month duration (January–June 2012) and was forced with six-hourly surface atmospheric conditions from the 0.14° ECMWF analysis starting in 2011. This OGCM experiment was performed in order to generate the initial conditions for the ocean in the AOGCM experiment and the SST and sea ice boundary conditions for the AGCM

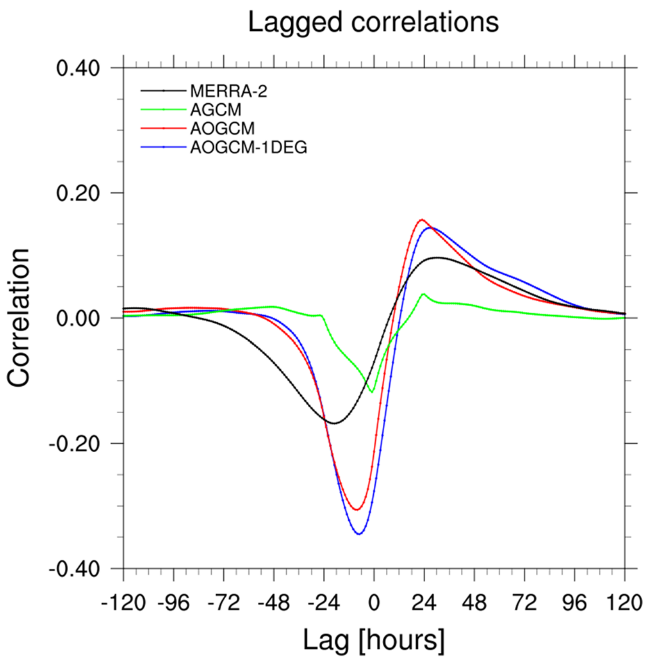

Figure 1. Lagged correlations between SST and wind speed tendencies between 50°, S to 50°, N. Positive lags correspond to SST leading the wind speed. The tendencies were calculated using the difference between two consecutive 24-h running means, offset by 1 h. AGCM = atmospheric general circulation model; AOGCM = atmosphere–ocean general circulation model; MERRA-2 = Modern Era Retrospective Reanalysis for Research and Applications Version 2.

experiment. The AGCM experiment was of 2-month duration (9 February to 9 April 2012). It was forced with SST and ice fraction from the OGCM, and initial conditions were taken from the Modern Era Retrospective Reanalysis for Research and Applications Version 2 (MERRA-2, Gelaro et al., 2017). The AOGCM experiment was of the same duration (9 February to 9 April 2012). The AOGCM ocean state was initialized from the OGCM experiment, and the atmosphere used the same initial conditions as the AGCM experiment (MERRA-2). An additional low-resolution AOGCM experiment was carried out, with nominal horizontal grid spacing of 1° and the same initial conditions as those used for the high-resolution experiment.

3. Results

In this study, we focus on daily time scales in order to exclude correlations enhanced by the diurnal cycle. No spatial high-pass filter was applied here, as was commonly done in previous studies, for example, Chelton and Xie (2010) & Bryan et al. (2010). We examine the difference between two successive days, referred to as the "tendency" rather than full fields (Booth et al., 2017; Wallace et al., 1988). In Figure 1 we show the 50°, S–50°, N averaged lagged correlation between tendencies of SST and tendencies of 10m wind speed for the high-resolution AOGCM and AGCM simulations, the low-resolution AOGCM (AOGCM-1DEG), and MERRA-2.

Our coupled system exhibits negative correlations at lags −1, 0 days (negative lag means wind leads SST) and positive correlations at lags 1, 2 days (SST leads wind). The AOGCM-1DEG simulation exhibits lagged correlations that are very similar to the higher resolution AOGCM experiment; however, the covariance in the AOGCM-1DEG simulation was found 30% smaller globally averaged suggesting a smaller amplitude oscillation. Unlike the AOGCM experiments, there is considerably less correlation in the AGCM simulation at any lag, and the negative correlation peak is shifted from negative lags to zero lag, suggesting that the strong AOGCM correlations are due to inherently coupled processes. At lag zero, some negative correlations are observed and may be attributed to the impact of the surface wind on the SST through the formulation of the atmosphere–ocean interface layer (see section 2). Similar to the coupled systems, MERRA-2 shows SST warming (cooling) at the same day and day after weaker (stronger) winds, and SST warming (cooling) a day or two before stronger (weaker) winds. The MERRA-2 correlations are weaker than the AOGCM correlations but stronger than the AGCM correlations. A possible explanation for this is that MERRA-2, being an atmosphere-only reanalysis, can only describe inherently coupled ocean–atmosphere processes when they are present in the assimilated observations. Positive correlations at lags 1, 2 suggest that the wind speed is lagging the SST by 1 to 2 days. Together with the negative correlations at lags −1, 0 this result suggests that there is a feedback cycle with a time scale of several days.

The amplitude of the tendencies of SST and wind speed were found to be non-negligible. For SST, the largest of the daily tendencies are larger than 0.5°C day^{-1}, with typical values in the range from 0.1°C day^{-1} to 0.3°C day^{-1}. These temperature tendencies extend down to the bottom of the ocean mixed layer (Figure 2). Daily tendencies of wind speed are often larger than 3 ms^{-1} day^{-1}. In many cases, turbulent flux variations during a cycle can reach 200 Wm^{-1} day^{-1}. The magnitude of these tendencies suggests that the oscillation is characterized by strong variability. An example of the magnitude of the variations for two locations is shown in Figure 2. The turbulent flux variations (top panels) often exceed 60 Wm^{-2} day^{-1}, wind speed variations (middle panels) are more than 3 ms^{-1} day^{-1} and ocean temperature variations (bottom panels) are larger than 0.2°C day^{-1} throughout the mixed layer. The figure also demonstrates a general behavior of SST cooling collocated with strong wind speed. Turbulent fluxes (latent heat plus sensible heat, positive upward) are positively correlated to the wind in general (no lag).

Figure 3 shows the spatial distribution of the correlations in the AOGCM, AGCM, and MERRA-2. For the AOGCM experiment the correlation between SST and wind speed tendency is in general negative for lags

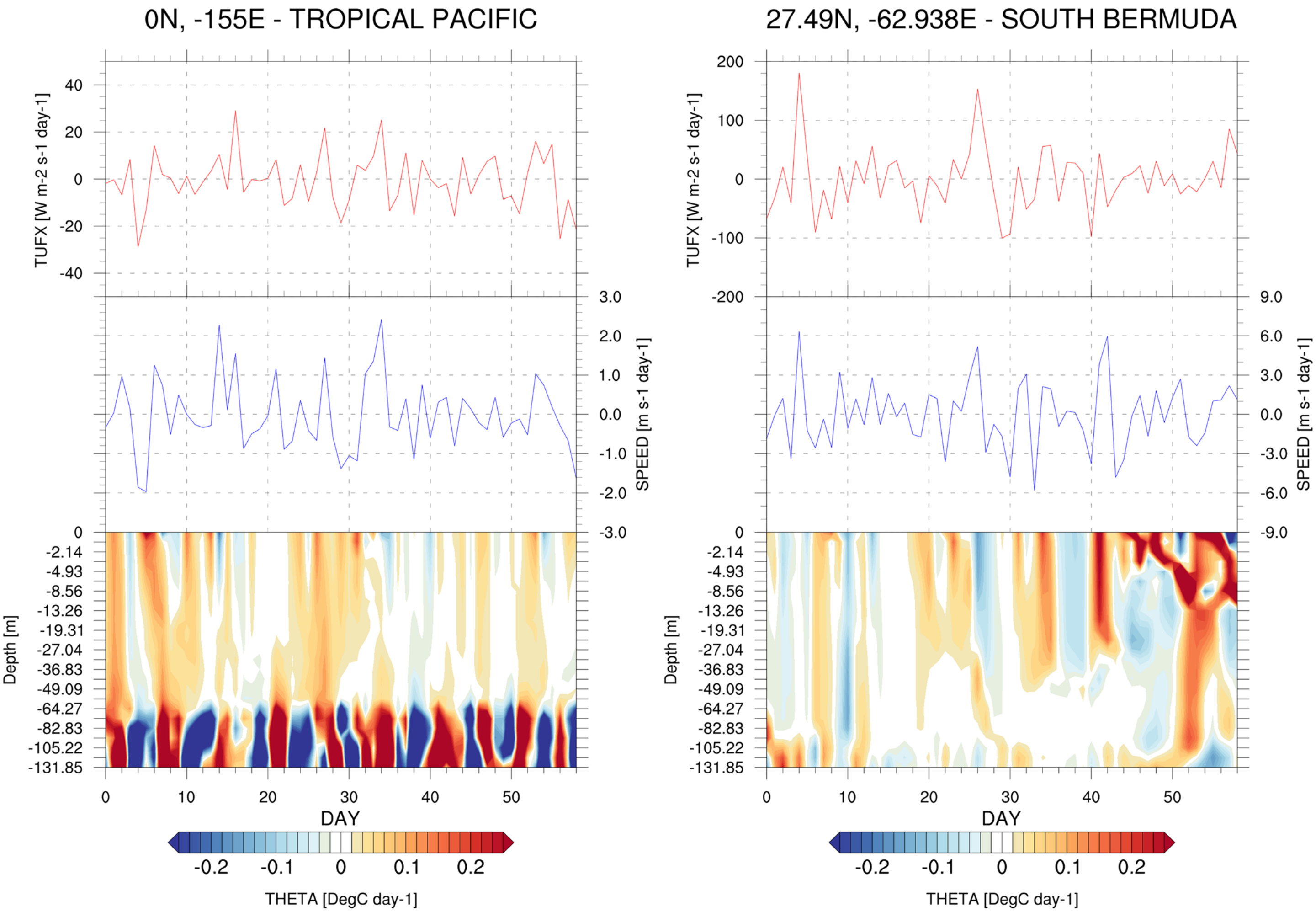

Figure 2. Daily tendencies in the tropical pacific (left) and south Bermuda (right) of turbulent fluxes (top), surface wind speed (middle), and ocean temperature at different levels (lower).

−1, 0 (first and second rows, respectively) and positive for lags 1, 2 (third and fourth rows) as seen in Figure 1. A significance test for the correlation was performed as suggested in Von Storch and Zwiers (1999). A cross spectral analysis of the SST and wind speed time series for each grid box showed a peak at a period ranging between 3 and 6 days for most of the globe (not shown).

The cyclic behavior is much less well defined in the AGCM experiment (green line in Figure 1 and middle panels of Figure 3). In Figure 3 it seems that the positive correlations exist in many regions, but the sign of the correlation is changing from one location to another. For example, the positive correlation at lag −1 day in the Eastern Pacific and in the Atlantic means that SST is lagging the wind at those locations. In MERRA-2 the lagged correlation pattern is more similar to the AOGCM in terms of the sign (negative at lags −1, 0 and positive at lags 1, 2) but the correlations are not statistically significant in many regions. The smaller correlations in MERRA-2 may be caused by the lack of an active ocean. Another possibility is that the diurnal cycle may play an important role in the correlation pattern, and MERRA-2 does not resolve the diurnal cycle of SST, as it is forced (in 2012) by daily mean SST data interpolated to the time step (Bosilovich et al., 2015).

The cyclic nature of SST and wind speed variations was also found in buoy data. Lagged correlations computed using data from three buoys in the tropical Pacific, three buoys at middle latitudes, and thwo buoys in the tropical Atlantic for the same time period as the GCM experiments are shown (Table 1, Figure 4). The oscillation pattern that was shown in Figure 1, suggesting a 3-to-6-day cycle, can also be found in the buoy data in all three regions, although it is somewhat weaker and noisier in the Atlantic. A weaker oscillation was also found in satellite-based observations by correlating surface winds from the cross-calibrated

10.1029/2019GL085837

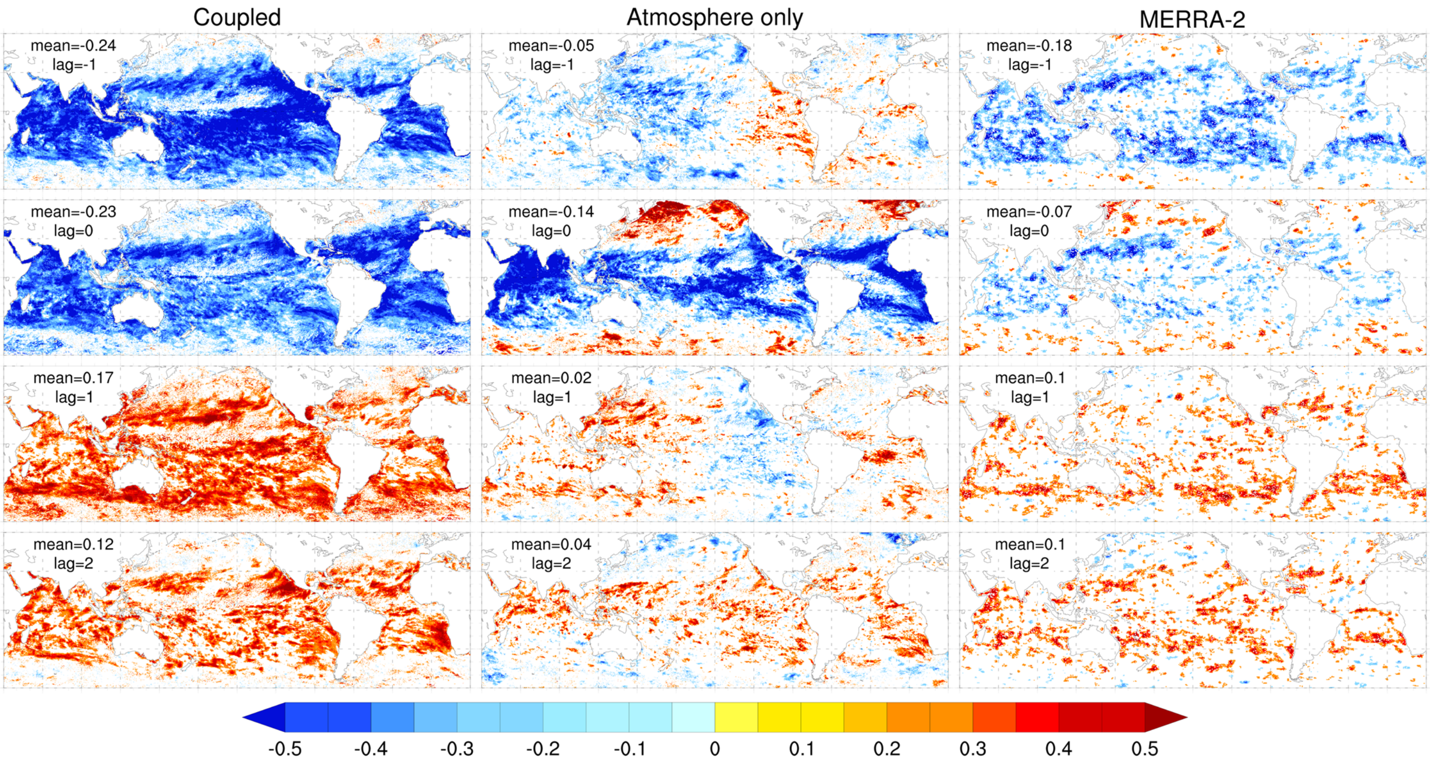

Figure 3. Correlations between SST tendency and wind speed tendency for -1,0,1 and 2 days for the AOGCM (left), AGCM (middle), and MERRA-2 (right). Positive lag corresponds to SST leading the wind speed. Non-significant grid boxes are colored white. MERRA-2 = Modern Era Retrospective Reanalysis for Research and Applications Version 2.

multi-platform (CCMP, Atlas et al., 2011) with SST from the optimally interpolated SST (OISST, Banzon et al., 2016).

4. Discussion and Concluding Remarks

Coupled atmosphere–ocean model (AOGCM) results were used here to compute lagged correlations between tendencies of surface wind speed and sea surface temperature. The pattern of negative correlation at lags of $-1, 0$ days together with positive correlation at lags of $1, 2$ days suggest a feedback or oscillation with a period of several days. In Figure 5 we propose a mechanism for the oscillation. If we start at the top of the schematic with a positive SST anomaly, the warmer water increases instability in the planetary boundary layer (PBL) and transfers more momentum from the upper levels to the surface. The resulting stronger wind speed at the surface (right side of schematic) increases upward latent and sensible heat fluxes and acts to cool the ocean surface (bottom of schematic). A cooler ocean increases stability and slows the transfer of

Table 1
Buoy Locations

name	lat	lon
TAOTRITON 1	$0°N$	$140°W$
TAOTRITON 2	$0°N$	$155°W$
TAO/TRITON 3	$0°N$	$170°W$
North Hawaii (WHOTS)	$23°N$	$158°W$
North Hawaii	$24°N$	$154°W$
West Atlantic	$27°N$	$63°W$
PIRATA 1	$20°N$	$38°W$
PIRATA 2	$19°S$	$34°W$

10.1029/2019GL085837

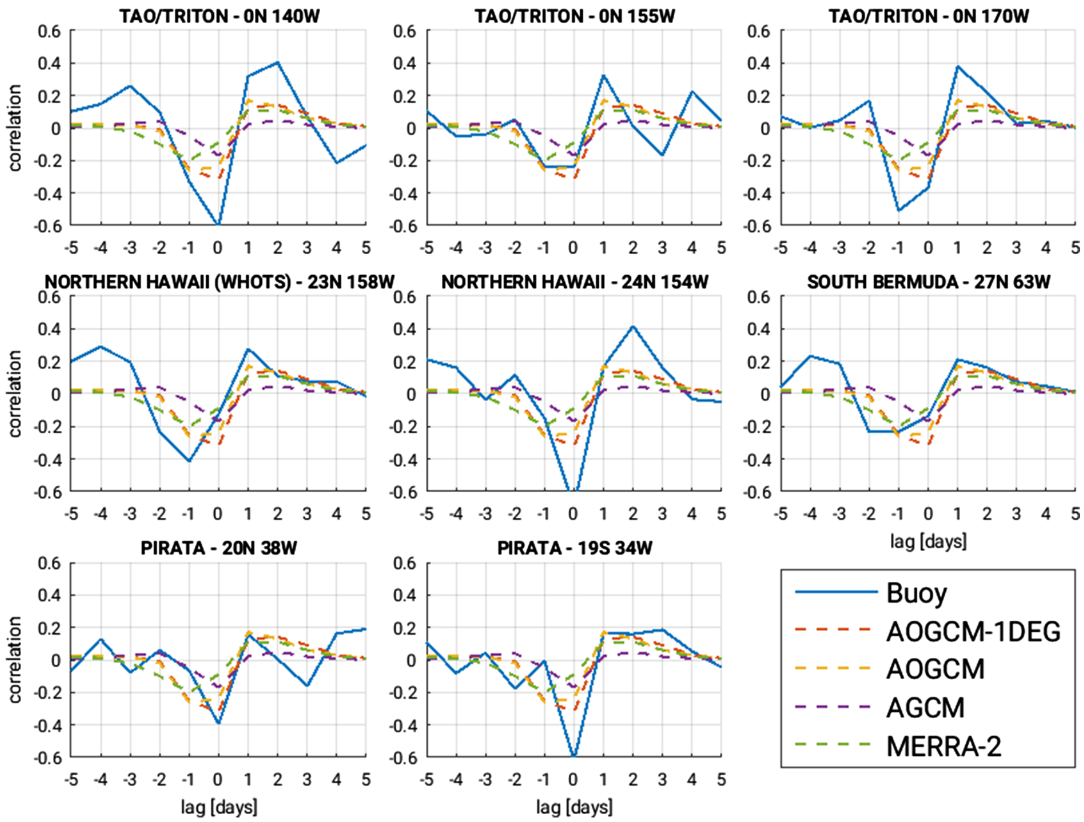

Figure 4. Lagged correlation between daily SST tendency and wind tendency from three tropical Pacific buoys (upper panels), three midlatitude buoys (middle panels), and two tropical Atlantic buoys (lower panels). The results are for the time period of this study: 9 February to 9 April 2012. Buoys lagged correlations are overlaid on the global AOGCM and AGCM lagged correlation patterns from Figure 1 (dashed). AGCM = atmospheric general circulation model; AOGCM = atmosphere–ocean general circulation model; MERRA-2 = Modern Era Retrospective Reanalysis for Research and Applications Version 2.

stronger winds to the surface. This reduces the wind (left panel of the schematic) and so the upward latent and sensible heat flux from the ocean resulting in a warmer ocean.

Correlations of SST with surface stability and turbulent fluxes (mainly through latent heat) were also found and reinforce the results of this study (supporting information Figures S2 and S3). Though less coherent in space and more sparse, SST was also found to correlate with atmospheric PBL height, cloud fraction, total precipitation, and convective precipitation, suggesting widespread impacts on the atmosphere above the PBL (Figures S4–S7). Misrepresentation of the oscillation in models, therefore, may have large implications on the large-scale atmospheric circulation through teleconnection patterns related to tropical convection and through changes of the wind patterns related to PBL height change.

The mechanism proposed in the schematic shown in Figure 5 exists globally, but there are regions where the mechanism is less spatially coherent. These regions are characterized by strong prevailing winds such as over the ACC. This may suggest that in those regions ocean up-welling and/or horizontal advection prevails. The correlation between SST tendency and wind speed tendency is strongest for SST greater than 16 °,C and wind speeds between 4 and 8 m s^{-1} (see Figure S8). Therefore regions of strong winds, for example, the midlatitude winter storm track have smaller correlation. The intensity of mesoscale eddies does not appear to play a significant role in modulating this 3-to-6-day oscillation since the correlation patterns are comparable for mesoscale eddy-admitting and non-eddying coupled simulations (compare left column of Figure 3 with Figure S9).

The low-resolution simulation also demonstrates the 3-to-6-day oscillation, similar to the high-resolution experiment, but some statistically significant differences between the high- and low-resolution simulations are found. The low-resolution simulation has slightly more negative correlation at negative lags and slightly less positive correlation at positive lags. The duration of the oscillation is also slightly longer in the low-resolution simulations as indicated by the small positive shift of the correlation peak at the positive lag

10.1029/2019GL085837

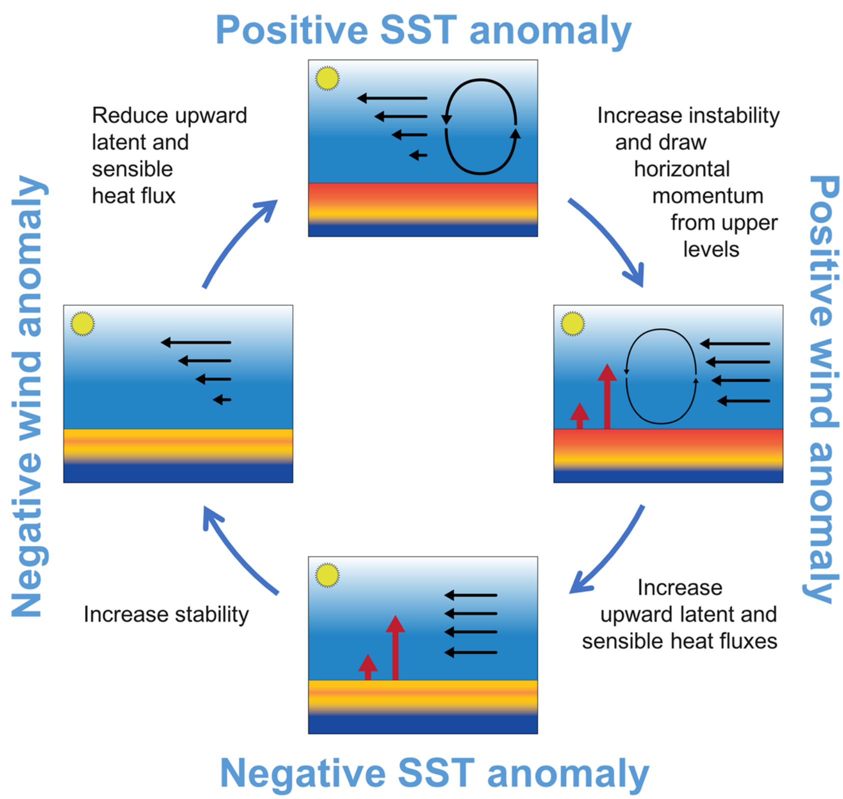

Figure 5. A suggested mechanism for the 3-to-6-day oscillation. SST = sea surface temperature.

in Figure 1. The extension of the positive correlations to longer lags in the low-resolution simulation may indicate that it takes more time for the wind to respond to changes in SST.

The time scale of this oscillation is longer than the turbulent time scale at the air–sea interface, and further study is required to determine what sets the time scale. It was found that the oscillations are not phase-locked with the daily cycle and so diurnal variations of solar heating and cooling do not set the time scale of the oscillations. The 3-to-6-day period may in part be set by a mechanism similar to a discharge oscillator (Jin, 1997), in which heat is being stored in the upper ocean and removed after several days. We have documented the presence of the 3-to-6-day oscillation in coupled models and in observations and plan to pursue the details of the mechanism in future studies.

Acknowledgments

The research leading to these results has received funding from the NASA Modeling, Analysis, and Prediction (MAP). Computations were carried out at the NASA Center for climate simulations (NCCS) at the NASA GSFC and the NASA High End Computing Capability (HECC) at NASA Ames. The authors acknowledge the Global Tropical Moored Buoy Array (GTMBA) Project Office of NOAA/PMEL for making the TAU/TRITON and PIRATA buoy observations publicly available. The authors acknowledge the National Data Buoy Center (NDBC) of NOAA for making the three midlatitude buoy observations publicly available. GF was supported by NASA award #6937342 and Simons Fundation award #549931. FAIR data standards data availability: Some of the model output data are presently available at: https://data.nas.nasa.gov/ecco/ and posting of the remaining data is underway. DM carried out research at the Jet Propulsion Laboratory, California Institute of Technology, under a contract with the National Aeronautics and Space Administration.

References

Adcroft, A., & Campin, J. M. (2004). Rescaled height coordinates for accurate representation of free-surface flows in ocean circulation models. *Ocean Modelling*, *7*(34), 269–284. https://doi.org/10.1016/j.ocemod.2003.09.003

Akella, S., Todling, R., & Suarez, M. (2017). Assimilation for skin SST in the NASA GEOS atmospheric data assimilation system. *Quarterly Journal of the Royal Meteorological Society*, *143*(703), 1032–1046. https://doi.org/10.1002/qj.2988

Alexander, M. A., Blad, I., Newman, M., Lanzante, J. R., Lau, N. C., & Scott, J. D. (2002). The atmospheric bridge: The influence of enso teleconnections on airsea interaction over the global oceans. *Journal of Climate*, *15*(16), 2205–2231. https://doi.org/10.1175/1520-0442(2002)015<2205:TABTIO>2.0.CO;2

Atlas, R., Hoffman, R. N., Ardizzone, J., Leidner, S. M., Jusem, J. C., Smith, D. K., & Gombos, D. (2011). A cross-calibrated, multiplatform ocean surface wind velocity product for meteorological and oceanographic applications. *Bulletin of the American Meteorological Society*, *92*(2), 157–174. https://doi.org/10.1175/2010BAMS2946.1

Balmaseda, M., Hernandez, F., Storto, A., Palmer, M., Alves, O., Shi, L., et al. (2015). The ocean reanalyses intercomparison project (ORA-IP). *Journal of Operational Oceanography*, *8*(sup1), s80–s97. https://doi.org/10.1080/1755876X.2015.1022329

Banzon, V., Smith, T. M., Chin, T. M., Liu, C., & Hankins, W. (2016). A long-term record of blended satellite and in situ sea-surface temperature for climate monitoring, modeling and environmental studies. *Earth System Science Data*, *8*(1), 165–176. https://doi.org/10.5194/essd-8-165-2016

Booth, J. F., Kwon, Y. O., Ko, S., Small, R. J., & Msadek, R. (2017). Spatial patterns and intensity of the surface storm tracks in CMIP5 models. *Journal of Climate*, *30*(13), 4965–4981. https://doi.org/10.1175/JCLI-D-16-0228.1

Bosilovich, M. G., Akella, S., Coy, L., Cullather, R., Draper, C., Gelaro, R., et al. (2015). MERRA-2: Initial evaluation of the climate. *Technical Report Series on Global Modeling and Data Assimilation*, *43*, 139. (NASA/TM201510).

Bryan, F. O., Tomas, R., Dennis, J. M., Chelton, D. B., Loeb, N. G., & McClean, J. L. (2010). Frontal scale air–sea interaction in high-resolution coupled climate models. *Journal of Climate*, *23*(23), 6277–6291. https://doi.org/10.1175/2010JCLI3665.1

Chelton, D. B., Esbensen, S. K., Schlax, M. G., Thum, N., Freilich, M. H., Wentz, F. J., et al. (2001). Observations of coupling between surface wind stress and sea surface temperature in the eastern tropical Pacific. *Journal of Climate*, *14*(7), 1479–1498. https://doi.org/10.1175/1520-0442(2001)014<1479:OOCBSW>2.0.CO;2

Chelton, D. B., & Xie, S. P. (2010). Coupled ocean-atmosphere interaction at oceanic mesoscales. *Oceanography*, *23*(4), 52–69.

Farneti, R., Delworth, T. L., Rosati, A. J., Griffies, S. M., & Zeng, F. (2010). The role of mesoscale eddies in the rectification of the southern ocean response to climate change. *Journal of Physical Oceanography*, *40*, 1539–1557.

Forget, G., Campin, J. M., Heimbach, P., Hill, C. N., Ponte, R. M., & Wunsch, C. (2015). Ecco version 4: An integrated framework for non-linear inverse modeling and global ocean state estimation. *Geoscientific Model Development*, *8*(10), 3071–3104. https://doi.org/10.5194/gmd-8-3071-2015

Foussard, A., Lapeyre, G., & Plougonven, R. (2019). Storm track response to oceanic eddies in idealized atmospheric simulations. *Journal of Climate*, *32*, 445–463.

Frenger, I., Gruber, N., Knutti, R., & Münnich, M. (2013). Imprint of southern ocean eddies on winds, clouds and rainfall. *Nature geoscience*, *6*(8), 608–612.

Garfinkel, C. I., Molod, A. M., Oman, L. D., & Song, I. S. (2011). Improvement of the GEOS-5 AGCM upon updating the air-sea roughness parameterization. *Geophysical Research Letters*, *38*, L18702. https://doi.org/10.1029/2011GL048802

Gelaro, R., McCarty, W., Surez, M. J., Todling, R., Molod, A., Takacs, L., et al. (2017). The modern-era retrospective analysis for research and applications, version 2 (MERRA-2). *Journal of Climate*, *30*(14), 5419–5454. https://doi.org/10.1175/JCLI-D-16-0758.1

Hashizume, H., Xie, S. P., Liu, W. T., & Takeuchi, K. (2001). Local and remote atmospheric response to tropical instability waves: A global view from the space. *Journal of Geophysical Research*, *106*(D10), 10,173–10,185. https://doi.org/10.1029/2000JD900684

Hayes, S. P., McPhaden, M. J., & Wallace, J. M. (1989). The influence of sea-surface temperature on surface wind in the eastern equatorial pacific: Weekly to monthly variability. *Journal of Climate*, *2*(12), 1500–1506. https://doi.org/10.1175/1520-0442(1989)002<1500:TIOSST>2.0.CO;2

Helfand, H. M., & Schubert, S. D. (1995). Climatology of the simulated great plains low-level jet and its contribution to the continental moisture budget of the United States. *Journal of Climate*, *8*(4), 784–806. https://doi.org/10.1175/1520-0442(1995)008<0784:COTSGP>2.0.CO;2

IPCC (2013). *Climate Change 2013: The physical science basis. Contribution of working Group I to the fifth assessment report of the Intergovernmental Panel on Climate Change*. Cambridge, United Kingdom and New York, NY, USA: Cambridge University Press.

Jin, F. F. (1997). An equatorial ocean recharge paradigm for enso. Part i: Conceptual model. *Journal of the Atmospheric Sciences*, *54*(7), 811–829. https://doi.org/10.1175/1520-0469(1997)054<0811:AEORPF>2.0.CO;2

Kirtman, B. P., Bitz, C., Bryan, F., Collins, W., Dennis, J., Hearn, N., et al. (2012). Impact of ocean model resolution on CCSM climate simulations. *Climate Dynamics*, *39*(6), 1303–1328. https://doi.org/10.1007/s00382-012-1500-3

Kuwano-Yoshida, A., & Minobe, S. (2017). Storm-track response to SST fronts in the northwestern pacific region in an AGCM. *Journal of Climate*, *30*, 1081–1102.

Large, W. G., McWilliams, J. C., & Doney, S. C. (1994). Oceanic vertical mixing: A review and a model with a nonlocal boundary layer parameterization. *Reviews of Geophysics*, *32*(4), 363–403. https://doi.org/10.1029/94RG01872

Liu, H., Li, W., Chen, S., Fang, R., & Li, Z. (2018). Atmospheric response to mesoscale ocean eddies over the south china sea. *Advances in Atmospheric Sciences*, *35*(9), 1189–1204. https://doi.org/10.1007/s00376-018-7175-x

Liu, T. W., Xie, X., Polito, P. S., Xie, S. P., & Hashizume, H. (2000). Atmospheric manifestation of tropical instability wave observed by QuikSCAT and tropical rain measuring mission. *Geophysical Research Letters*, *27*(16), 2545–2548. https://doi.org/10.1029/2000GL011545

Liu, W. T., Zhang, A., & Bishop, J. K. B. (1994). Evaporation and solar irradiance as regulators of sea surface temperature in annual and interannual changes. *Journal of Geophysical Research*, *99*(C6), 12,623–12,637. https://doi.org/10.1029/94JC00604

Ma, X., Chang, P., Saravanan, R., Montuoro, R., Hsieh, J. S., Wu, D., & Jing, Z. (2015). Distant influence of Kuroshio eddies on North Pacific weather patterns *Scientific Reports*, *5*, 17785.

Ma, X., Chang, P., Saravanan, R., Montuoro, R., Nakamura, H., Wu, D., et al. (2017). Importance of resolving Kuroshio front and eddy influence in simulating the North Pacific storm track. *Journal of Climate*, *30*, 1861–1880.

Ma, X., Jing, Z., Chang, P., Liu, X., Montuoro, R., Small, R. J., et al. (2016). Western boundary currents regulated by interaction between ocean eddies and the atmosphere. *Nature*, *535*(7613), 533.

Mantua, N. J., Hare, S. R., Zhang, Y., Wallace, J. M., & Francis, R. C. (1997). A pacific interdecadal climate oscillation with impacts on salmon production. *Bulletin of the American Meteorological Society*, *78*(6), 1069–1080. https://doi.org/10.1175/1520-0477(1997)078<1069:APICOW>2.0.CO;2

Marshall, J., Adcroft, A., Hill, C., Perelman, L., & Heisey, C. (1997). A finite-volume, incompressible Navier Stokes model for studies of the ocean on parallel computers. *Journal of Geophysical Research*, *102*(C3), 5753–5766. https://doi.org/10.1029/96JC02775

Matsueda, M., Mizuta, R., & Kusunoki, S. (2009). Future change in wintertime atmospheric blocking simulated using a 20-km-mesh atmospheric global circulation model. *Journal of Geophysical Research*, *114*, D12114. https://doi.org/10.1029/2009JD011919

Molod, A., Suarez, M., & Partyka, G. (2013). The impact of limiting ocean roughness on GEOS-5 AGCM tropical cyclone forecasts. *Geophysical Research Letters*, *40*, 411–416. https://doi.org/10.1029/2012GL053979

Molod, A., Takacs, L., Suarez, M., & Bacmeister, J. (2015). Development of the GEOS-5 atmospheric general circulation model: Evolution from MERRA to MERRA2. *Geoscientific Model Development*, *8*(5), 1339–1356. https://doi.org/10.5194/gmd-8-1339-2015

Okumura, Y., Xie, S. P., Numaguti, A., & Tanimoto, Y. (2001). Tropical Atlantic air-sea interaction and its influence on the NAO. *Geophysical Research Letters*, *28*(8), 1507–1510. https://doi.org/10.1029/2000GL012565

Price, J. F., Mooers, C. N. K., & Van Leer, J. C. (1978). Observation and simulation of storm-induced mixed-layer deepening. *Journal of Physical Oceanography*, *8*(4), 582–599. https://doi.org/10.1175/1520-0485(1978)008<0582:OASOSI>2.0.CO;2

Richter, I. (2015). Climate model biases in the eastern tropical oceans: Causes, impacts and ways forward. *Wiley Interdisciplinary Reviews: Climate Change*, *6*(3), 345–358. https://doi.org/10.1002/wcc.338

Rodwell, M. J., & Folland, C. K. (2002). Atlantic airsea interaction and seasonal predictability. *Quarterly Journal of the Royal Meteorological Society*, *128*(583), 1413–1443. https://doi.org/10.1002/qj.200212858302

Small, R., deSzoeke, S., Xie, S., O'Neill, L., Seo, H., Song, Q., et al. (2008). Air-sea interaction over ocean fronts and eddies. *Dynamics of Atmospheres and Oceans*, *45*(3), 274–319. OCEANIC FRONTS https://doi.org/10.1016/j.dynatmoce.2008.01.001

Strobach, E., Molod, A., Forget, G., Campin, J. M., Hill, C., Menemenlis, D., & Heimbach, P. (2018). Consequences of different air-sea feedbacks on ocean using MITgcm and MERRA-2 forcing: Implications for coupled data assimilation systems. *Ocean Modelling*, *132*, 91–111. https://doi.org/10.1016/j.ocemod.2018.10.006

Valdivieso, M., Haines, K., Balmaseda, M., Chang, Y. S., Drevillon, M., Ferry, N., et al. (2017). An assessment of air–sea heat fluxes from ocean and coupled reanalyses. *Climate Dynamics*, *49*(3), 983–1008. https://doi.org/10.1007/s00382-015-2843-3

Von Storch, H., & Zwiers, F. W. (1999). Statistical analysis in climate research (1st ed.). Melbourne, Australia: Cambridge University Press
Wallace, J. M., Lim, G. H., & Blackmon, M. L. (1988). Relationship between cyclone tracks, anticyclone tracks and baroclinic waveguides. *Journal of the Atmospheric Sciences*, *45*(3), 439–462. https://doi.org/10.1175/1520-0469
Wallace, J. M., Mitchell, T. P., & Deser, C. (1989). The influence of sea-surface temperature on surface wind in the eastern equatorial Pacific: Seasonal and interannual variability. *Journal of Climate*, *2*(12), 1492–1499.
Xie, S. P. (2004). Satellite observations of cool oceanatmosphere interaction. *Bulletin of the American Meteorological Society*, *85*(2), 195–208. https://doi.org/10.1175/BAMS-85-2-195
Zappa, G., Shaffrey, L. C., & Hodges, K. I. (2013). The ability of CMIP5 models to simulate North Atlantic extratropical cyclones. *Journal of Climate*, *26*, 5379–5396.
Zebiak, S. E. (1993). Airsea interaction in the equatorial Atlantic region. *Journal of Climate*, *6*(8), 1567–1586. https://doi.org/10.1175/1520-0442